bioRxiv preprint doi: https://doi.org/10.1101/724328; this version posted August 3, 2019. The copyright holder for this preprint (which was not certified by peer review) is the author/funder. All rights reserved. No reuse allowed without permission.

Title

Whole integration of neural connectomics, dynamics and bio-mechanics for identification of behavioral sensorimotor pathways in *Caenorhabditis elegans*

Authors

Jimin Kim[1], Julia A. Santos[2], Mark J. Alkema[3], Eli Shlizerman[1,2,*]
[1] Department of Electrical and Computer Engineering, University of Washington, Seattle, WA
[2] Department of Applied Mathematics, University of Washington, Seattle, WA
[3] Department of Neurobiology, University of Massachusetts Medical School, Worcester, MA
[*] Corresponding Author

Abstract

The ability to fully discern how the brain orchestrates behavior requires the development of successful computational approaches to integrate and inform in-vivo investigations of the nervous system. To effectively assist with such investigations, computational approaches must be generic, scalable and unbiased. We propose such a comprehensive framework to investigate the interaction between the nervous system and the body for the nematode *Caenorhabditis elegans (C. elegans)*. Specifically, we introduce a model that computationally emulates the activity of the *complete* somatic nervous system and its response to stimuli. The model builds upon the full anatomical wiring diagram, the *connectome,* and integrates it with additional layers including intra-cellular and extra-cellular bio-physically relevant neural dynamics, layers translating neural activity to muscle forces and muscle impulses to body postures. In addition, it implements inverse integration which modulates neural dynamics according to external forces on the body. We validate the model by in-silico injection of currents into sensory- and inter-neurons known to play a role in locomotion behaviors (e.g. posterior/anterior touch) and by applying external forces on the body. We are able to generate characteristic baseline locomotion behaviors (forward and backward movements). Inclusion of proprioceptive feedback, implemented through inverse integration, shows that feedback can entrain and sustain movements initiated by neural or mechanical triggers. We further apply neural stimuli, experimentally known to modulate locomotion, and show that our model supports natural behavioral responses such as turns, reversals and avoidance. The proposed model can be utilized to infer neural circuits involved in sensorimotor behavior. For this purpose, we develop large-scale computational ablation approaches such as (i) *ablation survey* and (ii) *conditional ablation*. Our results show how an ablation survey can identify neurons required for a ventral turning behavior. We also show how conditional ablation can identify alternative novel neural

bioRxiv preprint doi: https://doi.org/10.1101/724328; this version posted August 3, 2019. The copyright holder for this preprint (which was not certified by peer review) is the author/funder. All rights reserved. No reuse allowed without permission.

pathways, e.g. propose neurons which facilitate steering behavior towards olfactory attractants. The outcomes of our study show that the framework can be utilized to identify neural circuits, which control, mediate and generate natural behavior.

Keywords

Connectomics, neural dynamics, bio-mechanics, in-silico nervous system, Caenorhabditis elegans, proprioception

bioRxiv preprint doi: https://doi.org/10.1101/724328; this version posted August 3, 2019. The copyright holder for this preprint (which was not certified by peer review) is the author/funder. All rights reserved. No reuse allowed without permission.

Introduction

The nervous system controls and generates behavior. Circuits within the nervous system use rhythmic activity to facilitate coordinated body movements. How the information from stimuli is translated to movements and how movements shape neural responses is a fundamental question in neuroscience. Although Central Pattern Generator (CPG) networks, responsible for generating rhythmic neural activity and motor behavior, were found in various organisms, e.g., the locust, the lamprey, and recently in *C. elegans,* many details of sensorimotor integration and functional pathways guiding neural activity and movements are still to be resolved (1–3) . Computational approaches could assist with inference of such pathways by putting forward neural circuits candidates which mediate behaviors. Furthermore, computation could play a key role in analyzing the common principles of the interaction between the nervous system and the body.

In this respect, it is appealing to study the nematode organism *C. elegans* which spends most of its time in coherent sinusoidal wave locomotion. The nature of environmental stimuli (aversive or attractant) can lead to a change of locomotion direction. *C. elegans* wiring diagram, which maps electrical and chemical neural connections between all the neurons within its nervous system is completely resolved (4–9). The availability of the connectome warrants searching for incorporated circuits using computational and experimental techniques. While groups of sensory-, inter- and motor-neurons have been associated with various types of locomotion, it is still not fully resolved which sensorimotor mechanisms exist in *C. elegans* and which neural interactions form locomotion behaviors (10).

A central reason for the complexity stems from additional layers to the connectome. These layers encompass the biophysical dynamic processes representing neural responses and body bio-mechanics (11–16). These layers add numerous and intricate possibilities for signals to flow. Indeed, sensorimotor integration within *C. elegans* nervous system is likely to be highly recurrent and interactive through synapses, gap junctions, neuromodulators, body and proprioception (17). While it appears as an extremely complex system to study, the fact that these processes are coordinated during locomotion suggests that neural pathways guiding coordination could be inferred using computational approaches that effectively deal with the complexity (18, 19). Such approaches would aim to produce a model which includes dynamic layers along with the connectome to identify supported locomotion regimes. Beyond validation of locomotion, the power of integrating the layers is in the ability to break down the underlying

bioRxiv preprint doi: https://doi.org/10.1101/724328; this version posted August 3, 2019. The copyright holder for this preprint (which was not certified by peer review) is the author/funder. All rights reserved. No reuse allowed without permission.

neural circuits into functional pathways to inform experimental analyses. Furthermore, if designed correctly, such a platform has the potential to compile future details and *in vivo* findings into a developing model of the organism. To be a faithful platform it has to be modular, generic, scalable, effective and unbiased by specific behaviors or experiments.

C. elegans is the most suitable organism to aim to construct such a model. Availability of datasets and technological *in vivo* advances manipulating neural circuits indicate that a baseline platform for *C. elegans* is plausible (20). For that reason, we implement a computational three-pronged approach, which incorporates simulation of the nervous system as a dynamical network, translation of neural activity to muscle forces, and mapping muscle dynamics to *C. elegans* body model (Fig. 1). The framework allows to utilize methods such as posture dependent stimulation and ablation to discern behavioral neural pathways. These methods are inspired from experimental methods, however, the efficiency of the computational implementation enables their application on single and multiple cellular level through combinatorial surveys of the full nervous system and at any instance during locomotion behavior.

Previous approaches include modeling *C. elegans* body segmented as discrete rods controlled by stretch receptors and a subset of symmetric binary units mimicking ventral motor neurons. The model showed gaits generating forward locomotion but also instabilities when neurons dynamic properties and arrangement are slightly changed, e.g., when motor units replaced by neural dynamics, see (21) and references therein. Subsequent works also showed that pattern generators could be fit to produce forward locomotion (22). While these works show that oscillators can produce *C. elegans* forward locomotion body postures, their relation to the full nervous system and how these patterns are being generated remain unknown. Furthermore, a unifying relation to other locomotion behaviors such as backward, turns, pirouette movements remains unclear. Other line of work introduced a dynamical model for the complete somatic nervous system (23, 24). These works showed that the full nervous system is capable to generate rhythms even when a few mechano-sensory neurons received a simple constant stimulus. However, since additional layers of bio-mechanics and proprioception were not included, these rhythms could not be directly associated with behaviors. Inspired by the human brain project, the OpenWorm collaborative project was established in 2011 as a crowdsourcing platform aimed to develop generic bottom-up simulations of neuronal models, body and fluid simulations to lead to a full scale *C. elegans* model (9, 25). While there has been progress in development of generic tools for modeling *C. elegans* and other organisms, such as Geppetto

bioRxiv preprint doi: https://doi.org/10.1101/724328; this version posted August 3, 2019. The copyright holder for this preprint (which was not certified by peer review) is the author/funder. All rights reserved. No reuse allowed without permission.

(multiscale modeling) and Sibernetic (hydrodynamic simulation), integration of the different layers remains unapproached.

In this work we introduce a novel platform that overcomes the aforementioned challenges and is able to emulate the whole somatic nervous system and its response to stimuli along with the body of *C. elegans*. Our model integrates the full known somatic connectome, intracellular and extracellular neural dynamics, translates the activity of the nervous system to muscle forces which in turn generate body postures. In addition, it also implements inverse integration which modulates neural dynamics according to external forces on the body. The model does not rely on parameter fitting since connectivity is set by the connectome and neural interactions are set by biophysical properties of neural connections. The model is activated by either external neural stimuli (currents injected into neurons) and by external forces on the body. We test the model by comparing outcomes of body dynamics with *in vivo* experiments of touch responses which produce forward and backward movements and implement ablations found effective in those experiments. Furthermore, we perform further ablations to elucidate novel details on these experiments.

The power of our proposed platform is that it can unravel neural circuits involved in sensorimotor behavior. For this purpose, we develop large-scale computational ablation capabilities to infer neural pathways associated with various stimuli. These methods are inspired from experimental methods, however, the efficiency of the computational implementation enables their application on single and multiple cellular level through combinatorial surveys of the full nervous system and at any instance during locomotion behavior. Implementation of such approaches for the study of chemical sensation shows that we can identify alternative novel neural pathways, e.g., propose neurons which facilitate steering behavior towards olfactory attractants.

Results

We utilize the recently established computational neuronal network dynamical model of *C. elegans* to simulate responses of the nervous system to stimuli (22, 23, 26). This model is based on molecular properties of neurons in *C. elegans* network, as determined in experiments by modeling neural responses of the full somatic nervous system as: (i) graded potentials (ii) neural *gap* junctions connectivity (iii) neural dynamic *synaptic* connectivity including glutamergic, cholinergic and GABAergic receptors. Glutamergic and cholinergic transmitter activated ion channels are assumed to be excitatory as a first approximation. GABAergic receptors are

bioRxiv preprint doi: https://doi.org/10.1101/724328; this version posted August 3, 2019. The copyright holder for this preprint (which was not certified by peer review) is the author/funder. All rights reserved. No reuse allowed without permission.

assumed to be inhibitory as a first approximation. Notably, since our goal is to implement a baseline model, we do not fit the reversal potential values, however, values per channel, per specific connection, and the addition of more channels are easily configurable. These are part of plausible modifications to examine the effect of additional experimental details or hypotheses (27–30). We show an example of such variation by changing GABAergic channels to excitatory in forward locomotion. For more details see SM and (7, 8). The model incorporates parameters determined by the connectome and global biophysical conductance coefficients per type of connection. In addition, the model allows for computational clamping of neurons by external current injection. We previously observed that injection of constant current into sensory neurons, e.g., the posterior PLM mechanosensory neurons, evoke oscillatory neural responses in some motor neurons producing low dimensional attractor-like dynamics and transient dynamics with longer timescales than the intrinsic neural dynamics (24, 31).

In this work we investigate how the nervous system transforms its dynamics to behaviors by adding layers to the aforementioned model (Fig. 1A). These layers are necessary to explore how neural dynamics command and interact with the body. We connect motor neurons to muscles using experimentally determined map (9, 32). Notably, the spatial structure of the map is nontrivial and nonlocal (Fig. S6). We thereby physically model the musculature of *C. elegans* using a viscoelastic rod to resolve the relationship between motor neuron excitation and muscle activity. Such an approach was proposed for investigation of *eel* swimming with muscles activated by external signals emulating neural excitation (33, 34). In the framework, segments of the elastic rod (the body of the worm) are connected by joints, actuated by passive springs (correlating with gap junction between muscle segments), dashpots, and time-dependent force generators. Each muscle stimulation is determined by the calcium activity of motor neurons connected to it, and muscle contraction is represented in the rod as a force applied to a segment. The surrounding fluid and its effect on the moving rod is taken into account as an approximate framework (see SM for more details). We implement this model rather than the gaited model proposed for *C. elegans* (21), since it is based on body discretization into segments shown to be stable to neural stimulation and includes fluid environment modeling in the form of damping. In previous work, statistical models or synthetic muscle stimulation were used to generate body movements (21, 35, 36). Here we use the *complete* somatic nervous system simulation for such excitation. Neural voltage is translated to dorsal (D) and ventral (V) calcium transients, which in turn translate to muscle forces acting on body segments moving in two-dimensional space.

bioRxiv preprint doi: https://doi.org/10.1101/724328; this version posted August 3, 2019. The copyright holder for this preprint (which was not certified by peer review) is the author/funder. All rights reserved. No reuse allowed without permission.

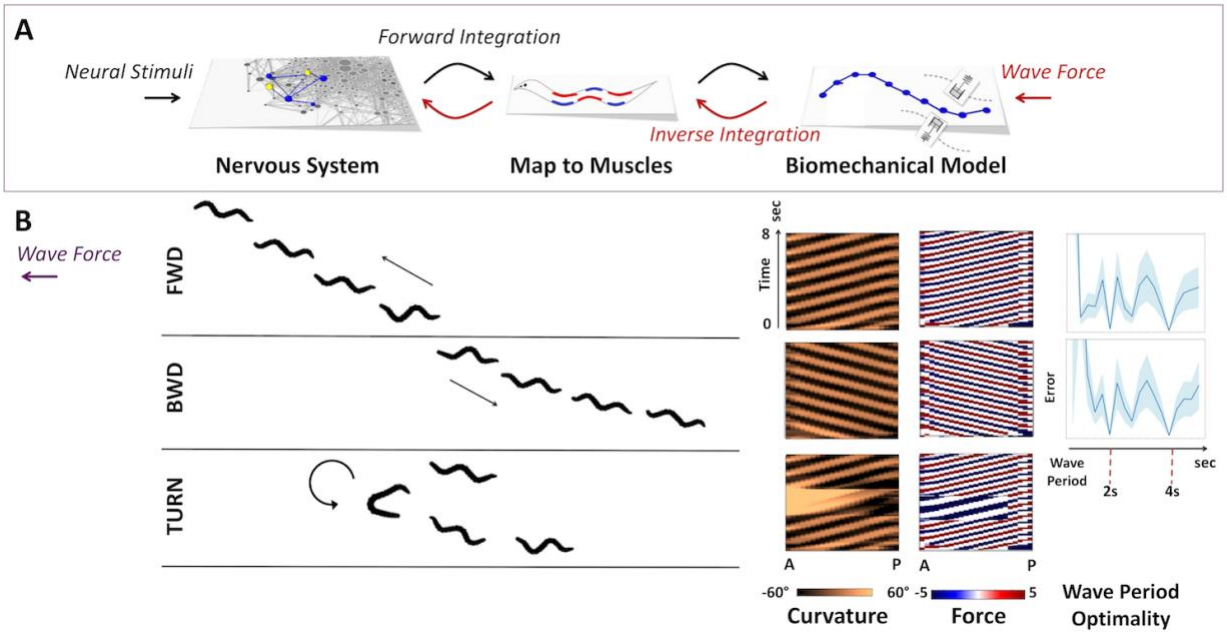

Figure 1: A: Layers in modeling *C. elegans* neuromechanical activity. Left to right: Layer 1: Modeling the nervous systems as a dynamical system encompassing the full somatic connectome including connectivity neural dynamics. Layer 2: Mapping neural dynamics to dynamic muscle impulses (forces). Layer 3: Muscle impulses are mapped to a biomechanical model that incorporates body responses and interaction with the environment. Neural stimuli are integrated forward to resolve body movements. External forces are propagated in an inverse direction to resolve corresponding neural dynamics. **B:** Typical locomotion patterns generated by three types of external wave forces, corresponding to forward (top), backward (middle), 180° turn (bottom) movements. The external force is inverse integrated to resolve neural dynamics, which are integrated forward to produces movements. Different wave periods of external force result in different 'preference' (i.e. the quantitative variance between initial and forward integrated external force) by neuronal network model. For forward and backward movement, the minimum variance is achieved when the wave period is 2s. Locomotion patterns are characterized using body snapshots, sampled every 2s, (left), curvature (middle) and muscle force (right). Also see SM Videos.

In addition to connecting the layers in feed forward manner, we developed an inverse integration approach, allowing us to infer neural dynamics from external force applied to the body. The approach transforms external forces acting on body to muscle activity and then inverts the activity to membrane voltages. These voltages are then integrated forward to resolve the body posture (see SM for more details). We use this approach to validate our model for three basic locomotion patterns: forward movement, backward movement and turn. For each pattern we design a force wave travelling along the body with variable frequency to infer neural dynamics associated with it. These neural dynamics are then forward integrated by the nervous system to generate the body posture. When we simulate the integration, we observe that

bioRxiv preprint doi: https://doi.org/10.1101/724328; this version posted August 3, 2019. The copyright holder for this preprint (which was not certified by peer review) is the author/funder. All rights reserved. No reuse allowed without permission.

generated movements can be almost indistinguishable from locomotion characteristics of freely moving animals (see SM Videos, snapshots, curvature maps, and calcium activity in Fig. 1). By measuring the error between the imposed traveling wave and the actual body curvature we observe that the nervous system includes preference for particular periods of the force, with optimal frequency being approximately 2 and 4s. These results indicate that the response of the nervous system is shaping the external force in a nontrivial and nonlinear manner (Fig 1B). Next we investigated the neural dynamics associated with these locomotion patterns. In Fig. 2A,B we show membrane voltage traces, in terms of difference from rest voltage, for the full somatic nervous system, and a group of 58 motor neurons part of the Ventral Nerve Cord (DB,VB, DA,VA,VD,DD) (see SM for additional neural voltage traces). We observe that the traces are consistent with activity patterns identified in the literature (37–40). The majority of the neurons are activated during locomotion. We find that (DB,VB) group is the most active group in forward locomotion and (DA,VA) group is the most active group in backward locomotion.

When we focus on (DB,VB) neurons and order them by their physical location along the anterior to posterior axis, we find that within each period of oscillation, the activity propagates with a preferred spatial direction (Fig. 2B black frames). During forward locomotion, voltage activity propagates from Anterior to Posterior (A->P) while for backward locomotion the propagation is from Posterior to Anterior (P->A). These propagation directions are consistent with the direction of movement (41, 42). Next we analyzed voltage responses using Singular Value Decomposition (SVD) to elucidate their characteristics. The SVD method decomposes the responses into spatial neuronal population modes (PC modes) and their temporal coefficients (23, 38, 43). We first apply SVD to understand the representation of each individual movement, in particular, we determine (i) the number of spatial modes needed to represent each activity and (ii) what is the complexity of the trajectories of the coefficients. The decomposition reveals that there are only a few (2-3) dominant spatial modes representing each movement and their associated dynamic coefficients follow a cyclic pattern (44). The success of the SVD method in revealing low-dimensionality leads us to seek for a unified basis of spatial neuronal modes, to

bioRxiv preprint doi: https://doi.org/10.1101/724328; this version posted August 3, 2019. The copyright holder for this preprint (which was not certified by peer review) is the author/funder. All rights reserved. No reuse allowed without permission.

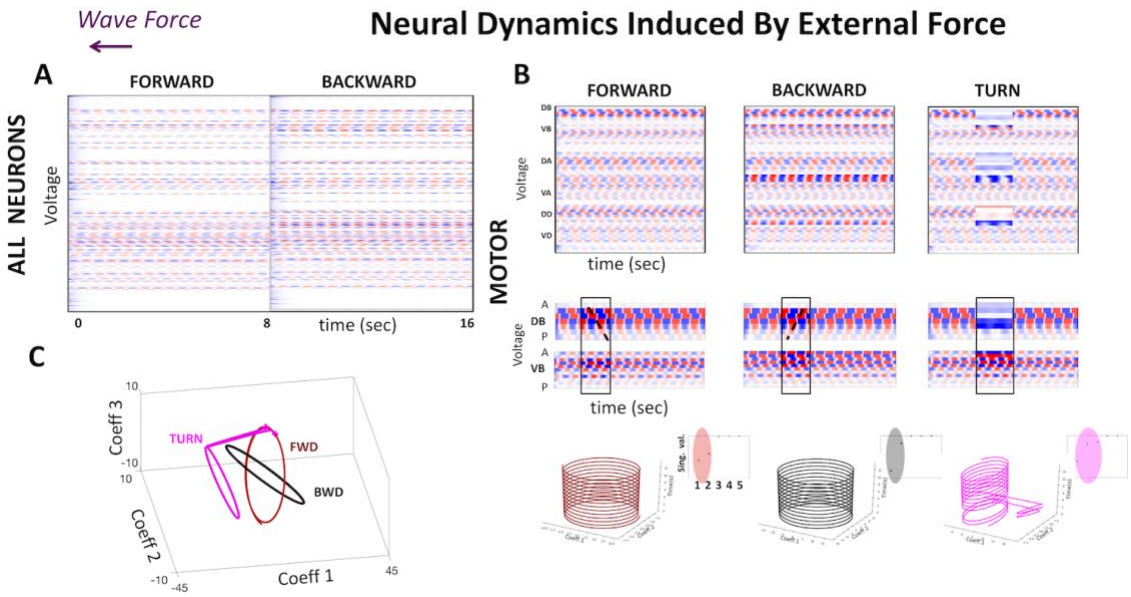

Figure 2: Neural responses of *C. elegans* somatic nervous system to external wave forces. **A**: Color raster plot of membrane voltage (difference from equilibrium) of 279 neurons inferred by back propagation of wave forces to corresponding neural dynamics. Neural responses generated for 16 sec: 0-8 sec: spatial wave force generating forward movement; 8-9:transition; 9-16 sec: spatial wave force generating backward movement. **B**: Color raster plots of membrane voltage of selected motor neurons for forward, backward and turn wave force profiles. Bottom row: SVD applied to all motor neurons; singular values and evolution of two temporal coefficients (associated with PC1 and PC2 respectively). **C**: Evolution of temporal coefficients during forward, backward and turn neural responses (red, black, magenta). Temporal coefficients are associated with PC modes from SVD analysis of all three responses (i.e. projected to a common space of PC1-PC3).

elucidate discriminative signatures of forward and backward movement (39). A viable candidate for such a basis is the set of first three PC modes obtained from SVD of all motor neurons voltages during forward, backward and turn movements. Projection of forward and backward responses onto this basis (PC space) yields cyclic temporal trajectories which are well separated and appear to be orthogonal (Fig. 2C). When projecting the turn voltage dynamics onto this space we observe that the trajectory departs from the forward cycle and approaches the region of the backward cycle. Notably, the PC space and the coefficients trajectories are obtained from the raw voltage dynamics and not from the derivative of calcium dynamics as described previously (39). This allows us to identify the PC space as a recognition space capable of determining the type and characteristics of movements the network performs from motor neural activity.

We next applied *neural clamping stimuli* to examine how they generate body movements. Notably, our goal is to explore movements created from simple constant stimuli where most of

bioRxiv preprint doi: https://doi.org/10.1101/724328; this version posted August 3, 2019. The copyright holder for this preprint (which was not certified by peer review) is the author/funder. All rights reserved. No reuse allowed without permission.

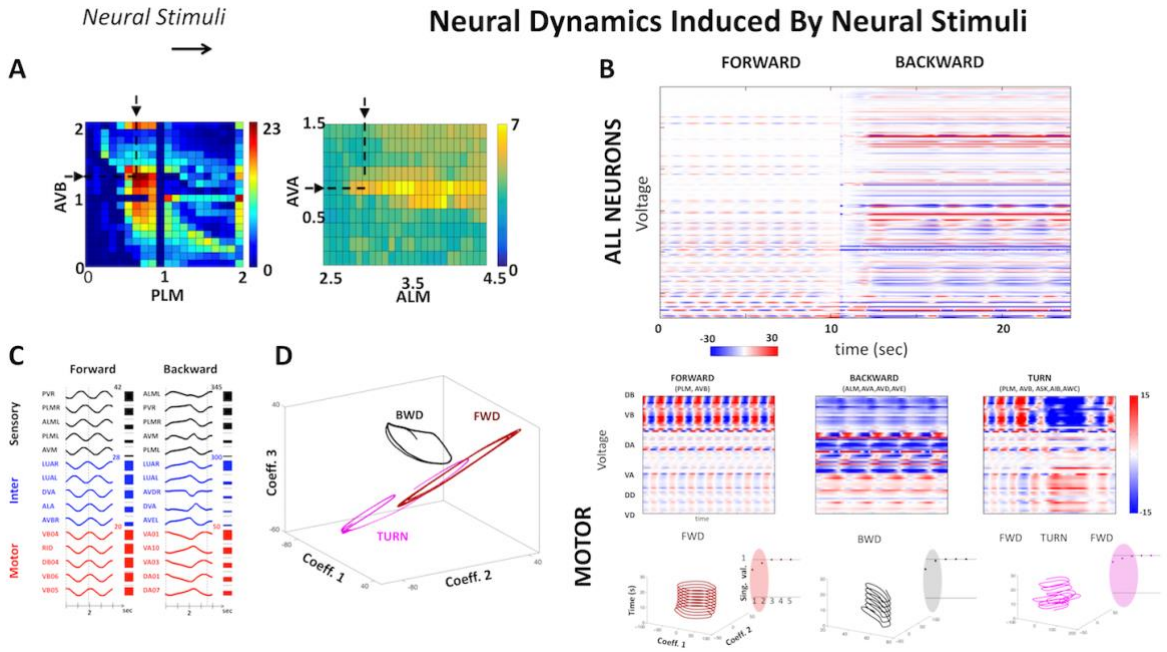

Figure 3: Simulated neural responses of *C. elegans* nervous system to external neural constant stimuli. **A**: Optimization over intensity of input current. The color encodes the distance passed by the body. Left: Stimulation of PLMR/L along with AVBR/L neurons emulating tail-touch response, which causes forward movement (optimum PLMR/L=0.7;AVBR/L=1.3). Right: Optimization of ALMR/L and AVAR/L input (optimum ALMR/L=2.6-2.9; AVBR/L=1) with fixed AVDR/L = 0.5, AVER/L=0.5 emulating backward movement (see SM). **B**: Top: Color raster plot of membrane voltage of optimal forward current; 10-15s:transition; 15-25s: optimal backward current. Middle: Color raster plots of membrane voltage of motor neurons for forward, backward and turn stimulations (compare with Figure 2A,B). Bottom row: SVD applied to all motor neurons; singular values and evolution of two temporal coefficients (associated with PC1 and PC2 respectively). **C**: Top 5 neurons (which have largest elements in PC1 mode) from each group (sensory, inter and motor) of neurons for forward (left) and backward (right) stimuli. **D**: Evolution of temporal coefficients during forward, backward and turn neural responses (red, black, magenta); compare with Figure 2C.

the neurons do not receive any input and no fitting is performed on baseline connectome parameters. When we inject constant current into randomly selected sensory- and inter-neurons we find a repertoire of stimuli producing oscillatory dynamics. However, these oscillations are variable and many of them are not associated with coherent directional locomotion. We therefore employ an optimization routine and target the circuits associated with touch response (37, 45, 46). The routine is set to find stimulations of sensory- and inter-neurons maximizing locomotion distance in either forward or backward directions. From neurons in this circuit, our simulations find a subset of both sensory- and inter-neurons related to behavioral responses: posterior-touch triggered forward locomotion (sens: PLM, inter: AVB or PVC), anterior touch triggered backward locomotion (sens: ALM, inter: AVA, AVD, AVE), and turn movement

bioRxiv preprint doi: https://doi.org/10.1101/724328; this version posted August 3, 2019. The copyright holder for this preprint (which was not certified by peer review) is the author/funder. All rights reserved. No reuse allowed without permission.

(sens:+ASK,AWC, inter:+AIB), see Fig. 3A, Fig. S3. The optimization shows that stimulation of sensory neurons alone could create rhythmic body curvatures but does not lead to forward and backward locomotion. Additional specific stimulation of interneurons is required to generate directed locomotion. This observation is consistent with experimental studies and control theory analysis (47, 48).

Voltage traces associated with neural clamping are consistent with voltage activity generated by spatially traveling wave; We observe similar active groups of motor neurons: (DB, VB) for forward, (DA, VA) for backward, a phase change in (DB, VB) in turn (Fig. 3C black frame), and similar preferred spatial direction in each period of oscillation. SVD analysis on voltage traces indicates occurrence of dimension reduction similarly to the body traveling wave force case. We selected the top five neurons from each neural group (sensory, inter, motor), which received the highest weight in the first PC mode, and display their membrane voltages over 4 sec time (Fig 3D). Strikingly, the selected neurons are those that are experimentally linked to forward and backward movements; for forward locomotion PLM, PVR sensory neurons and VB motor neurons, and for backward ALM, PLM sensory neurons and VA motor neurons. Furthermore, voltage responses time patterns are characteristic to the two different types of locomotion examined: for forward stimulus these are clear sinusoidal voltage dynamics with period of ~1.8sec in- and out-of-phase oscillations and for backward stimulus these are cusp like responses over longer period of ~3.4sec with two, in- and out, phases as well. These oscillations are not present in the stimulus and are generated by the intrinsic neural network interactions. Projection of forward and backward locomotion responses onto 3 PC modes embedding yields well separated cyclic trajectories as in the spatially traveling wave stimulation (Fig 3E). Similarly, turn voltage projected trajectory departs from the forward cycle and approaches the region of the backward cycle.

Experiments indicate that the environment plays a significant role in shaping coordinated movement (41, 49). We thereby explore environmental variations and their influence on *C. elegans* with respect to parameters such as viscosity and rod's elasticity, representing the ability

bioRxiv preprint doi: https://doi.org/10.1101/724328; this version posted August 3, 2019. The copyright holder for this preprint (which was not certified by peer review) is the author/funder. All rights reserved. No reuse allowed without permission.

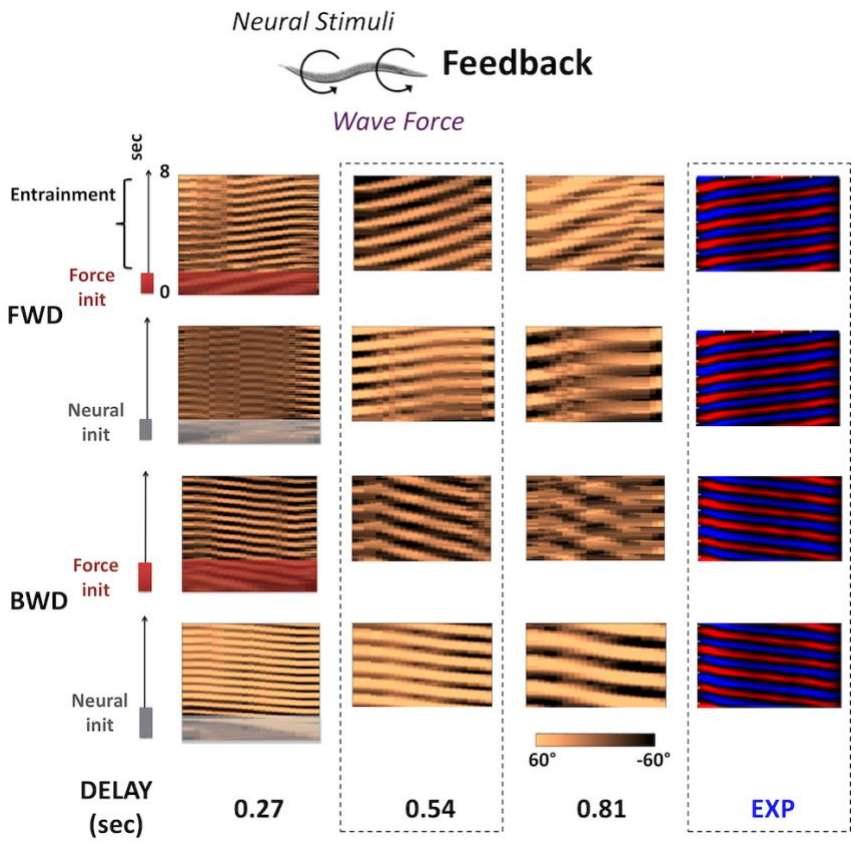

Figure 4: Proprioceptive feedback facilitates sustained locomotion. Feedback is initiated by a wave force (rows 1,3) or neural stimuli (rows 2,4) (see also SM Videos). Columns 1-3 display various feedback time delays, modeling the environmental reaction time of producing external forces on the body, and the curvature profiles they produce and compared to column 4, experimentally recorded curvatures (adapted from (42)). Time delay of approximately 0.5 sec produces optimal forward and backward locomotion which is close to experimental locomotion (highlighted by dashed border).

of the rod to propagate forces along the body (50). In all variations we fix the stimulus to optimal forward locomotion as characterized in Figs. 2,3. We observe that as the environment varies there are changes in the global characteristics of the movement (Fig. S9). Increasing viscosity values impedes movement by breaking off wave propagation from anterior to posterior, whereas decreasing them causes rapid extreme strokes unlike the body shapes seen in efficient *C. elegans* forward motion. When elasticity variations are added, these strokes intensify and create extremely atypical movements for high elasticity or no movement for low elasticity.

Proprioceptive *feedback* in which body movement drives neural activity may also occur. Experiments indicate that such mechanisms, e.g., proprioception within the motor neurons circuit, can facilitate locomotion and is an alternative to stimulation of command interneurons (36, 49, 51). To emulate proprioceptive feedback, we close the loop between neural stimulation

bioRxiv preprint doi: https://doi.org/10.1101/724328; this version posted August 3, 2019. The copyright holder for this preprint (which was not certified by peer review) is the author/funder. All rights reserved. No reuse allowed without permission.

and external body forces by inverse integrating the force that acts on the body to neural stimulation after a *time delay* (see SM for details) (52, 53). We test feedback effects by initiating locomotion with external stimulation, either neural current injection or spatial wave force. Once the feedback starts to entrain the movement we gradually turn external stimulation off. We find that in both initiation procedures feedback entrains the body into sustainable coherent movements in forward and backward directions such that the body moves solely due to feedback (Fig. 4; SM Videos). Variation in feedback delay time has an effect on coherency and we find the delay of approximately 0.5 sec to be closest to experimentally measured patterns (Fig. 4).

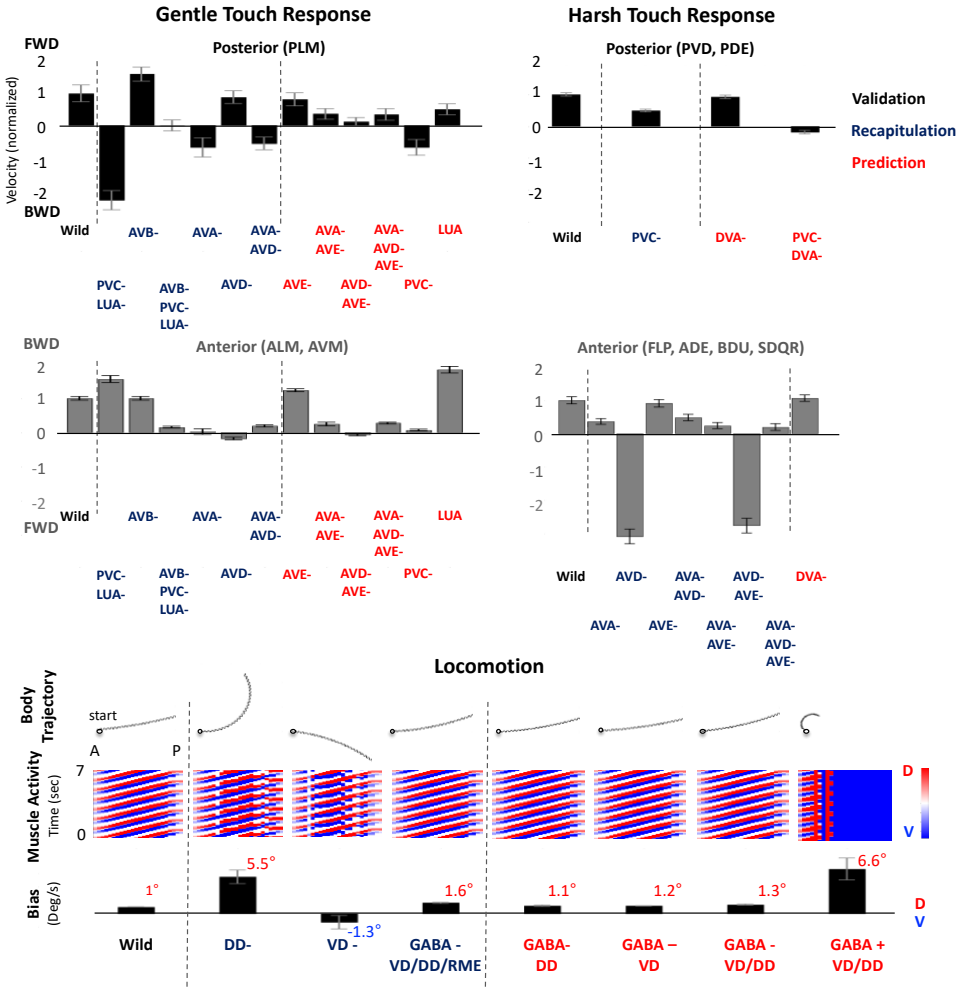

bioRxiv preprint doi: https://doi.org/10.1101/724328; this version posted August 3, 2019. The copyright holder for this preprint (which was not certified by peer review) is the author/funder. All rights reserved. No reuse allowed without permission.

Figure 5: Validation, recapitulation and prediction of locomotion behaviors for touch responses studied in-vivo. **A, B:** Body velocities for neural stimulation associated with **A:** Gentle (left) and Harsh (right) Posterior touch responses and **B:** Gentle (left) and Harsh (right) Anterior touch responses. Velocity amplitude is normalized according to the Wild (black label) locomotion and direction up is chosen as the expected direction. Recapitulated velocities following ablation experiments in (45, 54) (navy label) and Predicted ablations which were not performed in these experiments (red label) are compared to the Wild velocities. **C:** Body trajectory, muscle dynamics and bias from straight forward trajectory for external force stimulation and performing ablations as in-vivo (55) and predicted blocking and changing the sign of GABA channels.

We link neural stimulations with feedback and examine locomotion responses that were well studied in the literature, i.e. we focus on (i) *gentle* anterior or posterior touch (ii) *harsh* anterior or posterior touch. Neural and mechanical triggers for these behaviors have been identified and we use them to validate whether the model can produce the described behaviors (45, 54). We are able to validate that our model responds correctly to the appropriate stimulations by generating typical directional movement patterns (i) forward; during posterior touch neural stimulation (PLM (Gentle) and PVD+PDE (Harsh)) and (ii) backward; during anterior touch stimulation (ALM+AVM (Gentle) and FLP+ADE+BDU+SDQR (Harsh)), Fig. 5 A,B (Wild). Next, we perform ablation of neurons as done in the *in vivo* experiments, Fig. 5 A,B (Recapitulation). Our results are largely consistent with *in vivo* findings with some novel predictions from the model. Particularly, for PLM stimulation (Gentle Posterior), ablation of AVB or AVD does not hamper forward movement and even enhances it. PVC+LUA ablation causes the movement to reverse direction. Interestingly, we observe that AVA or AVA+AVD ablation also causes a reverse in direction. Such response was not described in the original experiment; however, recent experiments indicate involvement of AVA in forward movement (3). For ALM+AVM stimulation (Gentle Anterior) we observe that ablations of AVD or AVA are the most impactful. Ablation of AVA stops movement, while AVD ablation reverses it. Notably, effects of ablation are not simple nor additive, e.g., ablation of AVD alone is stronger than ablation of AVD and AVA; ablation of PVC, LUA and AVB causes the movement to almost stop while ablation of PVC, LUA or AVB separately permits forward movement. For PVD+PDE stimulation (Harsh Posterior) we observe that ablation of PVC does not lead to reverse in direction and for FLP+ADE+BDU+SDQR stimulation (Anterior Harsh) AVD or AVD+AVE ablation is found to reverse the direction from backward to forward. These observations are similar to those described in *in vivo* experiments.

Additional ablations could be performed to elucidate the obtained results. In the *in vivo* experiments, these were not perfromed due to technical challenges or other aspects, e.g., separate ablation of PVC and LUA was not possible in (45). Since in the model we can ablate

bioRxiv preprint doi: https://doi.org/10.1101/724328; this version posted August 3, 2019. The copyright holder for this preprint (which was not certified by peer review) is the author/funder. All rights reserved. No reuse allowed without permission.

any subset of neurons we perform these ablations (Fig. 5 A,B) (Prediction). For Posterior gentle touch, we identify the ablation of PVC alone as the most associated with a change in movement direction. We also observe that ablation of any combination of AVA, AVE, AVD does not lead to a change in movement direction compared to ablation of AVD alone. For Anterior gentle touch, we observe that ablation of PVC alone halts the movement, while ablation of LUA alone intensifies backward movement. These are interesting to compare with the recapitulated ablation of both PVC and LUA, which showed similar backward movement as the wild type indicating that when both neurons are ablated their effects are being cancelled out. For Posterior harsh touch, we observe that ablation of PVC along with DVA is capable to reverse the direction of movement, compared to PVC alone which did not change the direction. Furthermore, for Anterior harsh touch, ablation of DVA does not appear to play a role. We conclude the validation of the model by considering external wave force stimulation and ablation of subgroups of D motor-neurons (VD, DD) as in *in vivo* experiments (55). These experiments showed that while wild natural forward locomotion is mostly straight (with a slight dorsal bias), ablation of VD or DD motor-neurons introduced a directional bias: ablation of DD corresponded to locomotion with a dorsal bias, while ablation of VD corresponded to a ventral bias. Ablation of DD resulted with 4 times stronger bias than ablation of VD. We are able to produce similar results with our model, Fig. 5 C. Experiments also showed that blocking GABA in the whole nervous system (VD and DD are GABAergic neurons) does not introduce bias in the direction of the movement. We are able to confirm these results when we block all GABA receptors in the model. In addition, we blocked subsets of GABAergic receptors associated with each group (VD, DD, VD and DD), Fig. 5 C (Prediction). We observe that blocking any subset of them did not correspond to biases. The model incorporates further possibilities for circuit manipulations in addition to ablations and channel blocking. To demonstrate these abilities, we examine the effect of manipulating GABA VD and DD channels to be excitatory instead of inhibitory. Such manipulation turns out to generate an acute dorsal bias, see Fig. 5 C and SM Videos.

Investigation of basal locomotion in the model and comparison with *in vivo* investigations leads us to examine the effect of timed external stimuli impulses while the worm is performing basal locomotion. We first consider avoidance, which can be induced when forward locomotion is interrupted by ALM+AVM stimulus (55). *C. elegans* reacts to the change by stopping and reversing. We examine this scenario by initiating forward locomotion and after 6 sec applying ALM+AVM neural stimulation for 2 seconds. As we show in Fig. 6A, ALM+AVM neural stimulus is capable to generate the avoidance behavior; the stimulus disturbs forward locomotion and

bioRxiv preprint doi: https://doi.org/10.1101/724328; this version posted August 3, 2019. The copyright holder for this preprint (which was not certified by peer review) is the author/funder. All rights reserved. No reuse allowed without permission.

initiates backward locomotion. Inspection of neural activity of motor neurons (DB neurons are A->P ordered in Fig. 6A) indicates that the stimulus induces a change in the directionality of neural activity traveling wave from A->P to P->A. The transition is marked through high constant activity in the anterior motor-neurons.

In addition, we explore sharp ventral turns that occur during the reorientation in the direction of locomotion. The RIV motorneurons synapse onto ventral neck muscles and have been implicated in the execution of the ventral head bend (46, 56). To examine the role of RIV, we stimulate RIV neurons every 6 seconds for a duration of 3 seconds, while the worm is performing forward locomotion. As we show in Fig. 6B1, each RIV stimulus causes sharp ventral bend of the head leading to a rotation of forward locomotion course by approximately 90° while sustaining locomotion in the forward direction. Neural activity indicates that the turn corresponds to a bias added to the voltage activity of oscillating motor neurons. The rotation of the body is exhibited by two posture states: (i) neck straightening followed by a (ii) ventral turn. These states are observed in experimental studies of the escape response as well (55). We investigate these states by performing SVD on neural activity in each state and identify dominant neurons associated with the activity. We then compute the force magnitude resulting from dominant motor neurons activity (Fig. 6B2). We find that during neck straightening state, dorsal and ventral forces are well balanced and cancel each other out, while in the ventral turn state there is a strong ventral force acting on the muscle segments. Such analysis reveals neural participation on the cellular level in each state and how neural activity is superimposed to create particular posture.

bioRxiv preprint doi: https://doi.org/10.1101/724328; this version posted August 3, 2019. The copyright holder for this preprint (which was not certified by peer review) is the author/funder. All rights reserved. No reuse allowed without permission.

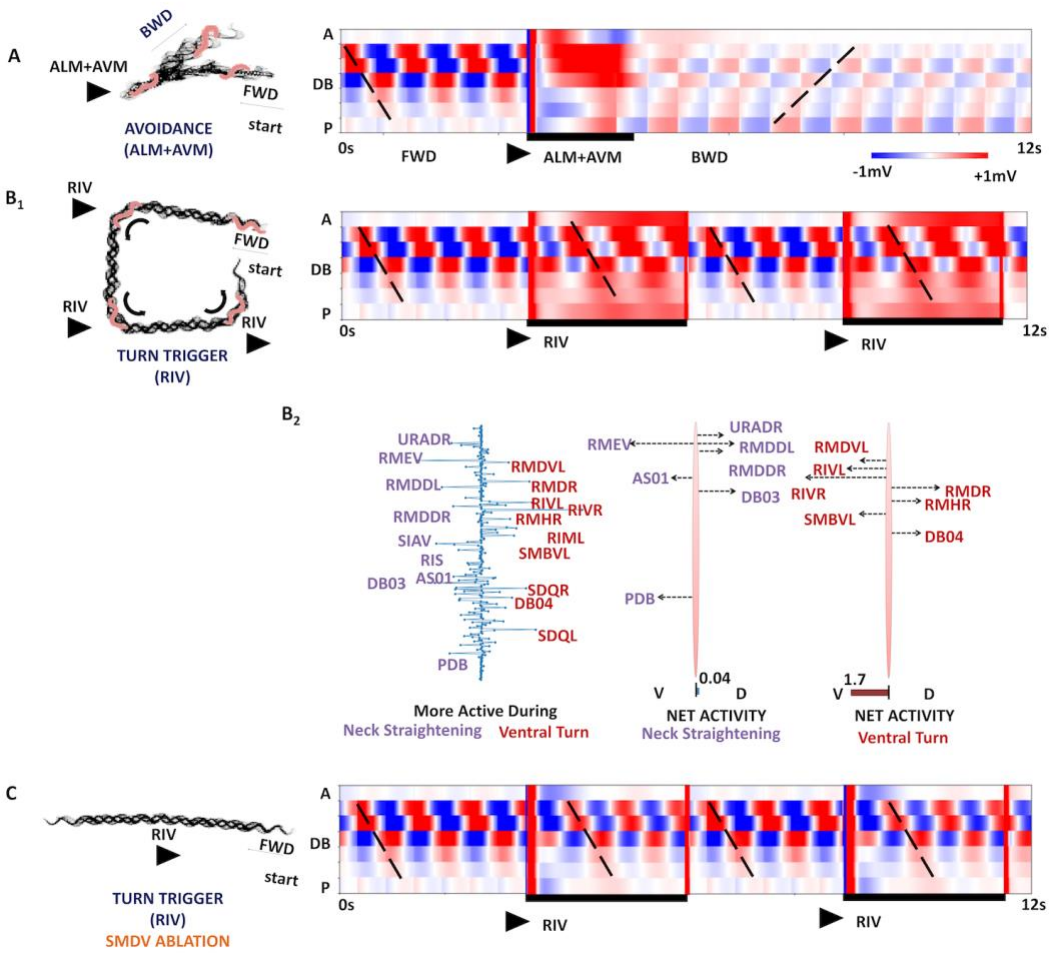

Figure 6: Neural impulses modify basal locomotion behavior. **A:** Avoidance behavior in which forward locomotion is interrupted by ALM+AVM impulse leading to backward locomotion (left: body posture histogram, right: motor neurons (DB) activity). **B_1:** RIV stimulus (2.7nA) is applied every 6 sec for duration of 3 sec during forward locomotion and rotates locomotion direction by 90°. **B_2**: Dominant neurons and forces involved in rotation of locomotion direction (left): (i) neck straightening-purple (ii) ventral turn-red. Middle: dominant motor neurons and corresponding forces they generate in ventral and dorsal directions (middle - neck straightening, right - ventral turn). **C:** The effect of SMDV ablation: typical RIV response (rotation by 90°) is disabled.

Since the model allows to perform structural neural ablations we utilize ablations to seek which neurons would be most correlated with this behavior. In particular, we select all pairs of neurons (R and L) from the group of neurons directly connected to RIV and separately ablate each pair. The analysis shows that the ablation of SMDV causes the most prominent change in the dynamics: the ablation disables the turn behavior and causes the body to continue with forward movement, see Fig. 6C1. Neural activity in the case of SMDV ablation is similar to neural

bioRxiv preprint doi: https://doi.org/10.1101/724328; this version posted August 3, 2019. The copyright holder for this preprint (which was not certified by peer review) is the author/funder. All rights reserved. No reuse allowed without permission.

activity during forward movement. These results suggest that both SMDV and RIV neurons are required to facilitate a sharp turn.

The success of triggering changes in movement by external stimuli and utilization of structural ablation suggests that these approaches can be used to examine sensory-neural-behavioral-environmental commands. In particular, these methods can be utilized to study how stimuli modulated by the posture of the body are “wired in” the network. For example, we examine the olfactory circuit of *C. elegans* subject to two `asymmetric neural stimuli’: stimulus is applied when (i) the head offset is in the dorsal direction (blue-dorsal) (ii) the head offset is in the ventral direction (red-ventral), Fig. 7 A,B. Such stimulus was implemented in-vivo through optogenetic stimulation and required precise timing between stimulus and posture (57, 58). We show that the model can be utilized to carry out such stimuli and we observe that the response is robust and anti-correlated to the direction of the head, i.e., blue-dorsal stimulus causes the head to turn in the ventral direction, while red-ventral stimulus causes the head to turn in the dorsal direction (Fig. 7C). Such function expresses steering away behavior and our results correspond to previously described *in vivo* quantifications (57, 58). On the cellular level we find stronger correlation and responses in *downstream* neurons (AIZ, RME, SMB) than in neurons on the *periphery* (AWC, AIY, AIB). Interestingly, stimulation of AWC alone does not produce either correlation/anti-correlation with the stimulus, however, when AWC stimulation is combined with AIY or AIB stimulation, it produces a robust anti-correlated response (Fig. 6A,C).

We employ a series of computational ablation studies to examine the neural pathways in the olfactory circuit. The AIZ interneuron provides a junction connecting sensory and downstream neurons. We therefore target the ablation to study AIZ, and upstream and downstream neurons from AIZ. We first consider activation of AIZ and ablate each neuron in the circuit. We find that ablation of downstream neurons (SMB or RME) indeed modify the motor response (marked by bold blue border). On the other hand, ablation of upstream sensory neurons (AWC, AIY and AIB) do not substantially modify the response with respect to the in-silico ‘wild’ worm (Fig. 8A).

bioRxiv preprint doi: https://doi.org/10.1101/724328; this version posted August 3, 2019. The copyright holder for this preprint (which was not certified by peer review) is the author/funder. All rights reserved. No reuse allowed without permission.

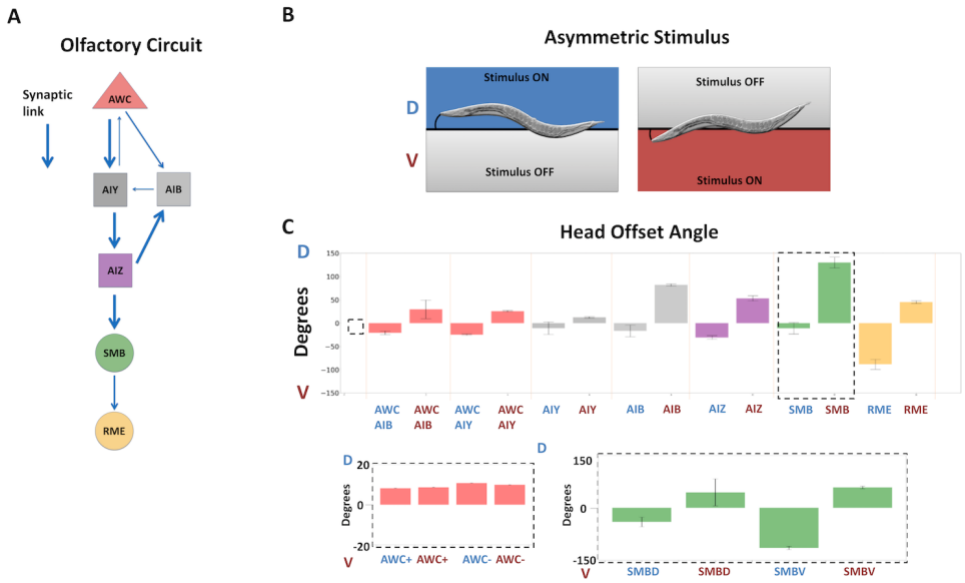

Figure 7: Olfactory circuit and head offset in response to 'asymmetric' posture aware stimulus. **A:** The olfactory circuit: arrows indicate synaptic connections and their width indicates synaptic strength. **B:** Two scenarios of the asymmetric stimulus are considered: Left: (i) stimulus is ON when horizonal angle of the head points in the dorsal direction (blue). Right: (ii) stimulus is ON when horizonal angle of the head points in the ventral direction (red). **C:** Response of neurons in the olfactory circuit to asymmetric stimulus (for each neuron, blue and red labels correspond to separate dorsal and ventral stimuli respectively) (top). Observed response is anti-symmetric. Inset bottom left - positive and negative asymmetric stimulation of AWC. Inset bottom right - selective asymmetric stimulation of SMB sub-groups (SMBV, SMBD).

To determine whether other neurons could be associated with the response we ablate each neuron from the interneurons group (86 neurons) and compare the induced motor responses. From that group we find that only a few (3) neurons capable to substantially modify the response (AIAL, RIS, AVKR). These neurons are potentially correlated with the olfactory processing response and could belong to the olfactory circuit as well.

As AIZ activation indicates that the pathway from AIZ is robust and downward directed, we stimulate upstream neurons to AIZ, i.e. AWC+AIY neurons, to test whether the peripheral stimulus flows exclusively through AIZ. Ablation survey of neurons in the olfactory circuit finds that ablation of AIY, SMB or RME modifies the response (marked by blue bold border), while remarkably AIZ ablation keeps the response intact (Fig. 8B left). This indicates that there are alternative routes transforming the stimulus from the periphery to motor neurons, which may be associated with *C. elegans* ability to respond in various ways to several odorants (59). We therefore perform a conditional ablation survey: we remove AIZ neuron from the network and survey ablation of another neurons from the interneurons group.

bioRxiv preprint doi: https://doi.org/10.1101/724328; this version posted August 3, 2019. The copyright holder for this preprint (which was not certified by peer review) is the author/funder. All rights reserved. No reuse allowed without permission.

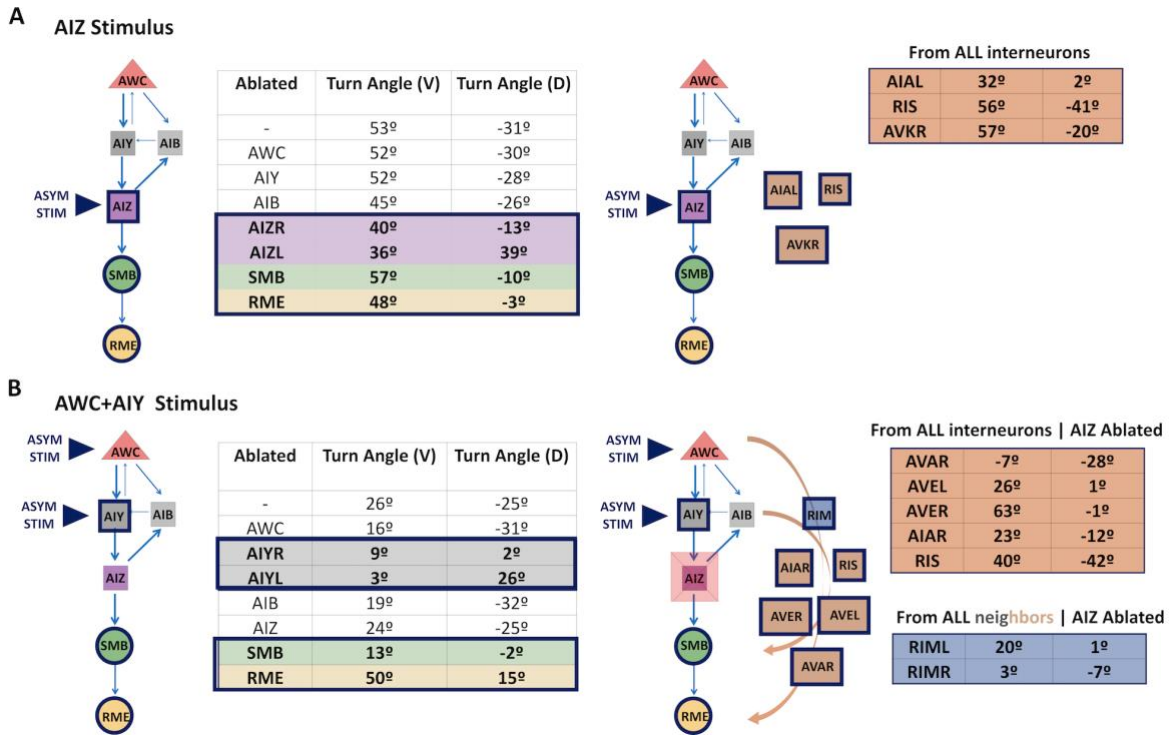

Figure 8: Computational ablation studies of the olfactory response. **A:** Asymmetric stimulus applied to AIZ in conjunction with ablation. Left: Table and circuit diagram summarizing the ablation of neurons from the olfactory circuit compared to healthy response. The first column indicates the ablated neuron. Significant deviation from healthy response is marked with blue border in the table and circuit diagram. Right: Ablation survey of all inter neurons proposes three additional neurons capable to modify the healthy response (orange shading). **B:** Asymmetric stimulus applied to periphery AWC+AIY with ablation of neurons from the olfactory circuit compared to healthy response. Left: Ablation of AWC, AIB, AIZ does not induce significant deviation from the healthy response. Right: Ablation survey of *all inter neurons* and *AIZ* (conditional ablation) suggests 5 neurons capable to modify the healthy response (orange shading). Ablation survey of all neighboring neurons (13) to AWC, AIY, AIB and 5 neurons found in previous step alongside AIZ. From that group RIM pair (blue shading) is found to be involved with the response and suggested as alternative junction to AIZ.

We find a sparse set of neurons (AVAR, AVER/L, AIAR, RIS) that modify the response (Fig. 8B2). These neurons indeed have direct and indirect connections to SMB or RME, however, are not directly connected to the stimulated AWC or AIY. Accordingly, we perform additional conditional ablation study to find possible junction neurons between them; We keep AIZ ablated and survey ablation of *neighboring* neurons connected to at least one neuron in the intersection set of AVAR, AVER/L, AIAR, RIS and AWC, AIY neurons. The intersection set includes 13

bioRxiv preprint doi: https://doi.org/10.1101/724328; this version posted August 3, 2019. The copyright holder for this preprint (which was not certified by peer review) is the author/funder. All rights reserved. No reuse allowed without permission.

neurons and we find that ablation of RIMR/L significantly alters the response. Indeed, RIMR and RIML, classified primarily as premotor neurons, have gap junctions connecting AIY with AVE, AVA and RIS. In conclusion, utilizing a sequential conditional ablation survey we are able to suggest that the olfactory circuit incorporates additional neurons capable to form alternative routes to transform olfactory signals from sensory to motor layers (Fig. 8A, B).

Conclusion

Our study provides a novel computational approach to explore the interaction between the nervous system and behavior in *C. elegans*. Our proposed model integrates neuromechanical layers composed of the connectome of the full somatic nervous system and its response to stimuli, effects of neural activity on body postures and proprioception. Our investigation is focused on studying locomotion circuits triggered by simple stimuli. Our analyses show that the structure of the connectome sets specific movement patterns enabled by neural dynamics and bio-mechanics.

We show that the transformations between the different layers are in the form of dynamic mappings (13, 15). These appear to be essential to determine whether neural activity is capable to generate coherent body movements and cannot be figured without full simulations. We introduce methods for forward integration (stimulus to muscles) and inverse integration (muscles to neural activity) allowing us to find correlation between neural stimuli and muscles and close the loop between them through feedback. We test the model by implementing spatially travelling wave forces along the body and find neural dynamics associated with them. Concurrently, we inject constant currents into neurons in the touch response circuit and observe that stimulation of a few neurons (sensory and inter neurons) in these circuits generates coordinated movements consistent with direction and patterns as in previous *in vivo* experiments. We then examine the effect of proprioceptive feedback and show that simple feedback with a time delay can entrain, smooth and sustain locomotion initiated by neural or external force stimuli. We further thoroughly test our model against previous touch response *in vivo* experiments which used ablations to identify key neurons implicated in the responses. We repeat these ablations and perform additional ablations, that were not performed in those studies, to further elucidate the roles of participating neurons in these circuits.

The validation of the results indicates that the dynamic layers within the model generate basal locomotion and related response behaviors. Since the incorporated layers are based on core

bioRxiv preprint doi: https://doi.org/10.1101/724328; this version posted August 3, 2019. The copyright holder for this preprint (which was not certified by peer review) is the author/funder. All rights reserved. No reuse allowed without permission.

anatomic structure and neural dynamics data, our results indicate that these processes are capable to generate locomotion and related responses. Additional information on the connectome, neural dynamics and processes such as monoamines signaling and neuropeptides activity modulation are rapidly become available (27–30). Moreover, modeling methodologies of the bio-mechanics are in process of being extended to three dimensions and continuous models (25, 60). Our model is constructed to support variations in bio-physical properties, layers and modeling methodologies. Investigations of the additional effects of such components could indicate behaviors and processes that are currently not included in the baseline model and to identify generative spontaneous behaviors. Furthermore, systematic inclusion of additional details in the model in the future could potentially allow for computational validation of conjectured novel processes and to explore development of the nervous system and body.

The success of the model to generate robust directional locomotion warrants the development of computational approaches utilizing the framework to identify functional neural circuits and pathways associated with specific neural stimuli. We demonstrate that such studies are plausible. We show how known circuits such as the touch responses can be studied in-depth using additional ablations yet performed or being impossible to perform *in vivo*. We also show examples of timed neural stimuli application during locomotion which give rise to variations in locomotion patterns and orchestrated behaviors. Specifically, we trigger behaviors such as avoidance and sharp turns through ALM+AVM and RIV neural impulses. We also induce steering behavior (also called weather vanning) through posture dependent asymmetric neural stimulation in the olfactory circuit. In addition, we demonstrate that ablation survey is capable to identify neurons participating in the sensorimotor pathway of these behaviors (e.g. SMDV neuron in RIV impulse pathway).

The outcomes of utilizing ablation directs us to implement approaches which scale the investigation to multiple instances and we apply them to study sensorimotor pathways in the olfactory circuit. We propose several types of ablation studies. (i) Ablation survey in which each neuron in a group of interest is ablated and the response is compared to the wild (unablated) one. Ablations that significantly modify the unablated behavior are proposed as potential candidates for inclusion in a sensorimotor pathway. We have identified such interneurons in the olfactory circuit. (ii) Conditional ablation in which a group of neurons is computationally removed from the circuit and ablation survey is performed on another group of neurons. Such study could

bioRxiv preprint doi: https://doi.org/10.1101/724328; this version posted August 3, 2019. The copyright holder for this preprint (which was not certified by peer review) is the author/funder. All rights reserved. No reuse allowed without permission.

assist in identification of alternate routes of neural processing. Indeed, previous *in vivo* studies identified multiple roles for interneurons in chemotaxis (59). We show that conditional AIZ ablation can identify alternate routes in the olfactory circuit. For these studies, the key component is the efficiency of the computational implementation which enables to perform surveys with numerous ablations on the full scale of the nervous system.

In conclusion, our observations indicate that functional sensorimotor pathways are intricate and include concurrent routes. The proposed computational model simulating all layers together in conjunction with comprehensive ablation studies could assist in identifying, enumerating and classifying sensorimotor pathways. Combination of such computational studies with empirical examination may extend our understanding of currently known neuromechanical functions and potentially lead to the unravelling of novel *C. elegans* brain circuits responsible for behaviors.

References

1. Goulding M (2009) Circuits controlling vertebrate locomotion: moving in a new direction. *Nat Rev Neurosci* 10(7):507–518.
2. Grillner S (1985) Neurobiological bases of rhythmic motor acts in vertebrates. *Science (80-)* 228(4696):143–149.
3. Gao S, et al. (2018) Excitatory motor neurons are local oscillators for backward locomotion. *Elife* 7:e29915.
4. Brenner S (2003) Nobel lecture: nature's gift to science. *Biosci Rep* 23(5):225–237.
5. Brenner S (1974) The genetics of Caenorhabditis elegans. *Genetics* 77(1):71–94.
6. J. G. White, E. Southgate, J. N. Thomson and SB (1986) The Structure of the Nervous System of the Nematode Caenorhabditis elegans. *Phil Trans R Soc Lond B*.
7. Varshney LR, Chen BL, Paniagua E, Hall DH, Chklovskii DB (2011) Structural properties of the Caenorhabditis elegans neuronal network. *PLoS Comput Biol* 7(2):e1001066.
8. Haspel G, O'Donovan MJ (2011) A perimotor framework reveals functional segmentation in the motoneuronal network controlling locomotion in Caenorhabditis elegans. *J Neurosci* 31(41):14611–14623.
9. Szigeti B, et al. (2014) OpenWorm: an open-science approach to modeling Caenorhabditis elegans. *Front Comput Neurosci* 8:137.
10. Bono M de, Villu Maricq A (2005) Neuronal substrates of complex behaviors in C. elegans. *Annu Rev Neurosci* 28:451–501.
11. McIntire SL, Jorgensen E, Kaplan J, Horvitz HR (1993) The GABAergic nervous system of Caenorhabditis elegans.
12. Bargmann CI (1998) Neurobiology of the Caenorhabditis elegans genome. *Science (80-)* 282(5396):2028–2033.
13. Kopell NJ, Gritton HJ, Whittington MA, Kramer MA (2014) Beyond the connectome: the dynome. *Neuron* 83(6):1319–1328.
14. Bargmann CI, Marder E (2013) From the connectome to brain function. *Nat Methods* 10(6):483.
15. Marder E (2011) Variability, compensation, and modulation in neurons and circuits. *Proc Natl Acad Sci* 108(Supplement 3):15542–15548.

bioRxiv preprint doi: https://doi.org/10.1101/724328; this version posted August 3, 2019. The copyright holder for this preprint (which was not certified by peer review) is the author/funder. All rights reserved. No reuse allowed without permission.

16. Stiefel KM, Brooks DS (2019) Why is There No Successful Whole Brain Simulation (Yet)? *Biol Theory* 14(2):122–130.
17. Lopez-Cruz A, et al. (2019) Parallel multimodal circuits control an innate foraging behavior. *Neuron*.
18. Pirri JK, McPherson AD, Donnelly JL, Francis MM, Alkema MJ (2009) A tyramine-gated chloride channel coordinates distinct motor programs of a Caenorhabditis elegans escape response. *Neuron* 62(4):526–538.
19. Maguire SM, Clark CM, Nunnari J, Pirri JK, Alkema MJ (2011) The C. elegans touch response facilitates escape from predacious fungi. *Curr Biol* 21(15):1326–1330.
20. DiLoreto EM, Chute CD, Bryce S, Srinivasan J (2019) Novel Technological Advances in Functional Connectomics in C. elegans. *J Dev Biol* 7(2):8.
21. Boyle JH, Berri S, Cohen N (2012) Gait modulation in C. elegans: an integrated neuromechanical model. *Front Comput Neurosci* 6:10.
22. Izquierdo EJ, Beer RD (2016) The whole worm: brain--body--environment models of C. elegans. *Curr Opin Neurobiol* 40:23–30.
23. Kunert J, Shlizerman E, Kutz JN (2014) Low-dimensional functionality of complex network dynamics: Neurosensory integration in the Caenorhabditis elegans connectome. *Phys Rev E* 89(5):52805.
24. Kunert-Graf JM, Shlizerman E, Walker A, Kutz JN (2017) Multistability and long-timescale transients encoded by network structure in a model of C. elegans connectome dynamics. *Front Comput Neurosci* 11. doi:10.3389/fncom.2017.00053.
25. Palyanov A, Khayrulin S, Larson SD (2018) Three-dimensional simulation of the Caenorhabditis elegans body and muscle cells in liquid and gel environments for behavioural analysis. *Philos Trans R Soc B Biol Sci* 373(1758):20170376.
26. Kim J, Leahy W, Shlizerman E (2019) Neural Interactome: Interactive Simulation of a Neuronal System. *Front Comput Neurosci* 13:8.
27. Liu Q, Kidd PB, Dobosiewicz M, Bargmann CI (2018) C. elegans AWA olfactory neurons fire calcium-mediated all-or-none action potentials. *Cell* 175(1):57–70.
28. Cook SJ, et al. (2019) Whole-animal connectomes of both Caenorhabditis elegans sexes. *Nature* 571(7763):63.
29. Bentley B, et al. (2016) The multilayer connectome of Caenorhabditis elegans. *PLoS Comput Biol* 12(12):e1005283.
30. Stern S, Kirst C, Bargmann CI (2017) Neuromodulatory control of long-term behavioral patterns and individuality across development. *Cell* 171(7):1649–1662.
31. Liu H, Kim J, Shlizerman E (2018) Functional connectomics from neural dynamics: probabilistic graphical models for neuronal network of Caenorhabditis elegans. *Philos Trans R Soc B Biol Sci* 373(1758):20170377.
32. WormAtlas N and, Altun ZF and, Hall D (2016) WormAtlas http://www.wormatlas.org. *WormAtlas*. Available at: http://www.wormatlas.org.
33. McMillen T, Holmes P (2006) An elastic rod model for anguilliform swimming. *J Math Biol* 53(5):843–886.
34. McMillen T, Williams T, Holmes P (2008) Nonlinear muscles, passive viscoelasticity and body taper conspire to create neuromechanical phase lags in anguilliform swimmers. *PLoS Comput Biol* 4(8):e1000157.
35. Sznitman R, Gupta M, Hager GD, Arratia PE, Sznitman J (2010) Multi-environment model estimation for motility analysis of Caenorhabditis elegans. *PLoS One* 5(7):e11631.
36. Wen Q, et al. (2012) Proprioceptive coupling within motor neurons drives C. elegans forward locomotion. *Neuron* 76(4):750–761.
37. Piggott BJ, Liu J, Feng Z, Wescott SA, Xu XZS (2011) The neural circuits and synaptic mechanisms underlying motor initiation in C. elegans. *Cell* 147(4):922–933.
38. Kato S, Xu Y, Cho CE, Abbott LF, Bargmann CI (2014) Temporal responses of C.

bioRxiv preprint doi: https://doi.org/10.1101/724328; this version posted August 3, 2019. The copyright holder for this preprint (which was not certified by peer review) is the author/funder. All rights reserved. No reuse allowed without permission.

elegans chemosensory neurons are preserved in behavioral dynamics. *Neuron* 81(3):616–628.
39. Kato S, et al. (2015) Global brain dynamics embed the motor command sequence of Caenorhabditis elegans. *Cell* 163(3):656–669.
40. Nguyen JP, et al. (2016) Whole-brain calcium imaging with cellular resolution in freely behaving Caenorhabditis elegans. *Proc Natl Acad Sci* 113(8):E1074--E1081.
41. Pierce-Shimomura JT, et al. (2008) Genetic analysis of crawling and swimming locomotory patterns in C. elegans. *Proc Natl Acad Sci* 105(52):20982–20987.
42. Xu T, et al. (2018) Descending pathway facilitates undulatory wave propagation in Caenorhabditis elegans through gap junctions. *Proc Natl Acad Sci* 115(19):E4493--E4502.
43. Shlizerman E, Schroder K, Kutz JN (2012) Neural activity measures and their dynamics. *SIAM J Appl Math* 72(4):1260–1291.
44. Stephens GJ, Johnson-Kerner B, Bialek W, Ryu WS (2008) Dimensionality and dynamics in the behavior of C. elegans. *PLoS Comput Biol* 4(4):e1000028.
45. Chalfie M, et al. (1985) The neural circuit for touch sensitivity in Caenorhabditis elegans. *J Neurosci* 5(4):956–964.
46. Gray JM, Hill JJ, Bargmann CI (2005) A circuit for navigation in Caenorhabditis elegans. *Proc Natl Acad Sci U S A* 102(9):3184–3191.
47. Fang-Yen C, Alkema MJ, Samuel ADT (2015) Illuminating neural circuits and behaviour in Caenorhabditis elegans with optogenetics. *Phil Trans R Soc B* 370(1677):20140212.
48. Yan G, et al. (2017) Network control principles predict neuron function in the Caenorhabditis elegans connectome. *Nature* 550(7677):519.
49. Li W, Feng Z, Sternberg PW, Xu XZS (2006) A C. elegans stretch receptor neuron revealed by a mechanosensitive TRP channel homologue. *Nature* 440(7084):684–687.
50. Backholm M, Ryu WS, Dalnoki-Veress K (2013) Viscoelastic properties of the nematode Caenorhabditis elegans, a self-similar, shear-thinning worm. *Proc Natl Acad Sci* 110(12):4528–4533.
51. Sawin ER, Ranganathan R, Horvitz HR (2000) C. elegans locomotory rate is modulated by the environment through a dopaminergic pathway and by experience through a serotonergic pathway. *Neuron* 26(3):619–631.
52. More HL, Donelan JM (2018) Scaling of sensorimotor delays in terrestrial mammals. *Proc R Soc B Biol Sci* 285(1885):20180613.
53. Tytell ED, Hsu C-Y, Williams TL, Cohen AH, Fauci LJ (2010) Interactions between internal forces, body stiffness, and fluid environment in a neuromechanical model of lamprey swimming. *Proc Natl Acad Sci* 107(46):19832–19837.
54. Li W, Kang L, Piggott BJ, Feng Z, Xu XZS (2011) The neural circuits and sensory channels mediating harsh touch sensation in Caenorhabditis elegans. *Nat Commun* 2:315.
55. Donnelly JL, et al. (2013) Monoaminergic orchestration of motor programs in a complex C. elegans behavior. *PLoS Biol* 11(4):e1001529.
56. Albrecht DR, Bargmann CI (2011) High-content behavioral analysis of Caenorhabditis elegans in precise spatiotemporal chemical environments. *Nat Methods* 8(7):599.
57. Kocabas A, Shen C-H, Guo Z V, Ramanathan S (2012) Controlling interneuron activity in Caenorhabditis elegans to evoke chemotactic behaviour. *Nature* 490(7419):273.
58. Kotera I, et al. (2016) Pan-neuronal screening in Caenorhabditis elegans reveals asymmetric dynamics of AWC neurons is critical for thermal avoidance behavior. *Elife* 5:e19021.
59. Bargmann CI, Hartwieg E, Horvitz HR (1993) Odorant-selective genes and neurons mediate olfaction in C. elegans. *Cell* 74(3):515–527.
60. Cohen N, Ranner T (2017) A new computational method for a model of C. elegans

bioRxiv preprint doi: https://doi.org/10.1101/724328; this version posted August 3, 2019. The copyright holder for this preprint (which was not certified by peer review) is the author/funder. All rights reserved. No reuse allowed without permission.

biomechanics: Insights into elasticity and locomotion performance. *arXiv Prepr arXiv170204988*.